THE ASTROPHYSICAL JOURNAL, 435:L55–L58, 1994 November 1

FAR-ULTRAVIOLET IMAGING OF THE GLOBULAR CLUSTER NGC 6681 WITH WFPC2[1]

ALAN M. WATSON,[2] JEREMY R. MOULD,[3] JOHN S. GALLAGHER III,[2] GILDA E. BALLESTER,[4]
CHRISTOPHER J. BURROWS,[5] STEFANO CASERTANO,[6] JOHN T. CLARKE,[4] DAVID CRISP,[7]
RICHARD E. GRIFFITHS,[6] J. JEFF HESTER,[8] JOHN G. HOESSEL,[2] JON A. HOLTZMAN,[9]
PAUL A. SCOWEN,[8] KARL R. STAPELFELDT,[7] JOHN T. TRAUGER,[7]
AND JAMES A. WESTPHAL[10]

Received 1994 May 16; accepted 1994 August 11

ABSTRACT

We have imaged the globular cluster NGC 6681 in the far-UV and visible with WFPC2 on the *HST*. Our far-UV images show a sparsely populated and fully resolved central region, and we detect 122 stars. The far-UV to visible color-magnitude diagram shows a well-defined horizontal branch with no evidence for hot, more evolved descendants. We find one hot horizontal-branch star significantly below the model zero-age horizontal branch, but the rest are consistent with evolutionary models within uncertainties in calibration, distance, and reddening. The center of the cluster harbors two luminous blue stragglers. Our far-UV images graphically confirm that there is no steep density gradient at small radii among the horizontal-branch stars of this post–core-collapse cluster and show no evidence for significant color gradients.

Subject headings: globular clusters: individual: (NGC 6681) — stars: evolution — stars: horizontal-branch — ultraviolet: stars

1. INTRODUCTION

The hot stellar content of globular clusters provides many clues to the post–main-sequence evolution of low-mass stars. The zero-age position of a star on the horizontal branch (HB) is determined by uncertain details of its evolution on the red giant branch, including mass loss. The evolutionary paths available after leaving the HB are even more complex, yet stars in these very late stages are likely to be the principal contributors to the far-UV excess in nearby E and S0 galaxies and spiral bulges (see O'Connell 1993).

In this *Letter* we describe far-UV observations of the globular cluster NGC 6681 with the second Wide Field and Planetary Camera (WFPC2) on the *Hubble Space Telescope*. We present a preliminary study of the structure of the hot HB in a far-UV to visible color-magnitude diagram and the far-UV and visible radial profiles.

The Ultraviolet Imaging Telescope (UIT) demonstrated that imaging in the far-UV is a powerful tool in the study of hot stars in globular clusters (Hill et al. 1992; Landsman et al. 1992; Smith et al. 1993; Parise et al. 1994; Whitney et al. 1994). Far-UV observations are required because of the insensitivity of visible colors at high temperatures. UIT and WFPC2 are complementary instruments. WFPC2 has a small field (2.′7), superb resolution (0.″1 FWHM in the visible and 0.″2 FWHM in the far-UV), and CCD detectors; UIT has a large field (40′), coarse resolution (typically 3.″1 FWHM), and uses intensified photocathodes with film. These characteristics make WFPC2 better suited for the construction of accurate color-magnitude diagrams even into the centers of globular clusters, but allows UIT to completely survey clusters for stars in luminous but short-lived post-HB phases.

NGC 6681 is also known as M70. It is a prototypical post–core-collapse cluster, whose radial profile is thought to be better characterized by a power law than a King model (Djorgovski & King 1984). It has a currently accepted distance modulus (DM) of 14.82 ± 0.2, placing it about 2 kpc from the Galactic Center, has a low reddening with $E_{B-V} = 0.06 \pm 0.02$, and has intermediate metallicity with [Fe/H] $= -1.51$ (Peterson 1993; Zinn & West 1984). NGC 6681 was observed with *ANS* by van Albada, de Boer, & Dickens (1981) and classified as extremely blue (EB) on the basis of its integrated UV color. This characterization was confirmed by Caloi et al. (1984) using *IUE*. These authors also noted that the far-UV light was smoothly distributed and not dominated by a single bright star.

2. DATA

2.1. *Observations and Reductions*

Exposures of 1500 and 700 s were taken in F160W and a single 100 s exposure was taken in F555W on 1994 March 3 and 4. WFPC2 images the sky onto four 800 × 800 CCDs at pixel scales of 0.″046 (PC1) and 0.″100 (WF2, WF3, and WF4). The cluster center was located on WF2. See Burrows (1994) and Trauger et al. (1994) for further details of the instrument. The images were reduced following Holtzman et al. (1994) and the two F160W images were combined using a standard cosmic-ray rejection algorithm. Images in both bands of the central 25.″6 × 25.″6 of the cluster are shown in Figure 1 (Plate L26).

[1] Based on observations with the NASA/ESA *Hubble Space Telescope*.

[2] Department of Astronomy, University of Wisconsin–Madison, 475 North Charter Street, Madison, WI 53706.
[3] Mount Stromlo and Siding Springs Observatories, Australian National University, Private Bag, Weston Creek Post Office, ACT 2611, Australia.
[4] Department of Atmospheric, Oceanic, and Space Sciences, University of Michigan, 2455 Hayward, Ann Arbor, MI 48109.
[5] Astrophysics Division, Space Science Department, ESA and Space Telescope Science Institute, 3700 San Martin Drive, Baltimore, MD 21218.
[6] Department of Astronomy, Johns Hopkins University, 3400 North Charles Street, Baltimore, MD 21218.
[7] Jet Propulsion Laboratory, 4800 Oak Grove Drive, Pasadena, CA 91109.
[8] Department of Physics and Astronomy, Arizona State University, Tyler Mall, Tempe, AZ 85287.
[9] Lowell Observatory, Mars Hill Road, Flagstaff, AZ 86001.
[10] Division of Geological and Planetary Sciences, California Institute of Technology, Pasadena, CA 91125.

F160W is a sodium Woods filter produced at JPL and has a wide bandpass from 1300 to 1900 Å. The precise response is uncertain to some degree, but the red tail of the filter is significantly steeper than the preliminary curve given by Burrows (1994), and so we have truncated that curve at 2050 Å. Its excellent blocking properties are demonstrated by the complete absence of detectable light from even the brightest cluster giants in the F160W images. The measured FWHM in the F160W images is about 0".19 near the center of each of the WF chips, but away from the center of each chip the PSF is radially elongated and has an ellipticity of up to about 0.3, probably as a result of chromatic aberration in the MgF_2 field flatteners. F160W introduces significant vignetting beyond 80". F555W is a wide V filter. The measured FWHM in the F555W images is about 0".15 on the WFs and better than 0".1 on PC1, and the PSF does not vary significantly across the field. Unfortunately, the brightest stars in the F555W image are saturated in the WFs. The exposures were taken with the CCDs at $-76°$ C, and as such suffer from a small vertical charge transfer inefficiency (Trauger et al. 1994).

2.2. *Calibration*

Zero points were calculated from 1994 March 8 observations of GRW $+70°5824$, a DA3 white dwarf spectrophotometric standard (Turnshek et al. 1990). We use $m \equiv -2.5 \log \langle f_\lambda \rangle - 21.1$, where $\langle f_\lambda \rangle \equiv \int Q_\lambda T_\lambda f_\lambda \lambda \, d\lambda / \int Q_\lambda T_\lambda \lambda \, d\lambda$ and the units of $\langle f_\lambda \rangle$ are ergs s^{-1} cm^{-2} $Å^{-1}$. The STSDAS spectrum and responses $Q_\lambda T_\lambda$ from Burrows (1994), modified as above, give $m_{160} = 9.26$ and $m_{555} = 12.74$ with an uncertainty in the far-UV flux and hence m_{160} of about 10%. Measurement errors were about 4% in F160W and 2% in F555W.

WFPC2 underwent a standard decontamination on 1994 February 22, several days prior to our observations. From observations of the UV flux monitor BD $+75°375$ we calculate that the average throughput in F160W at the time of our observations of NGC 6681 was approximately 2% higher than the throughput at the time of the observations of GRW $+70°5824$. Structure in the deposition of contaminants has been found, so the reduction will vary between and across chips by perhaps 1%.

If we adopt an $R_V = 3.2$ reddening law from Cardelli, Clayton, & Mathis (1989), the interstellar reddening of $E_{B-V} = 0.06 \pm 0.02$ corresponds to $A_{160} = 0.52$ and $A_{555} = 0.19$. If the reddening is nonstandard, A_{160} may differ from this value.

The combined systematic errors other than in extinction are ~ 0.23 in $(m - M)_{160}$, from a combination of uncertainties in distance and the zero point, 0.21 in $(m - M)_{555}$, largely from uncertainties in distance, and 0.12 in $(m - M)_{160} - (m - M)_{555}$, largely from uncertainties in the zero point of m_{160}.

2.3. *Photometry*

A total of 122 stars were detected in F160W. Of these, 18 were unsuitable for photometry because they fell on CCD defects (eight), suffered vignetting or were too close to the edge of the field or the pyramid shadow (four), or were very close neighbors (six). A further 46 were saturated in F555W, leaving 58 with good magnitudes in both filters.

Photometry was performed using apertures of radius 0".5 for F160W and 0".2 for F555W, with encircled energy fractions of 0.83 and 0.80. The large aperture used for F160W ensured that the variable PSF did not introduce field-dependent errors into the photometry and to confirm this we repeated the photometry with apertures as large as 1".0. The small aperture used for F555W was dictated by the moderately crowded nature of these images.

Most of the 46 stars saturated in F555W were saturated in their central pixel only. We were able to obtain useful limits on m_{555} by noting that the value in the saturated pixel must lie between the ADC saturation level (about 50,000 electrons) and the physical full well (about 85,000 electrons, according to Gilliland 1994). This procedure failed for one star with a very bright neighbor. The resulting photometry is good to about 10%.

Contributions to random errors in addition to Poisson noise arise from the flats (2%), variable deposition of contaminants (1% in m_{160}), and the vertical charge transfer inefficiency (up to 3% RMS). This leads to total random errors for unsaturated HB stars of about 5% in m_{160} and 4% in m_{555}.

A far-UV to visible color-magnitude diagram (CMD) of NGC 6681 is shown in Figure 2. The most striking feature of the CMD is the HB. We have carefully checked the reality of outliers. Saturation in the F555W frame begins at about $m_{555} \approx 16.0$. Most of the HB stars cooler than about 10,000 K are saturated, but the two blue straggler candidates are not. We have added artifically dimmed stars to the images to determine a magnitude limit in F160W of $m_{160} \approx 18.1$, at which point the stars become confused with coincident cosmic-ray events. This limit is marked with a dashed line in the CMD.

3. THE HOT HORIZONTAL BRANCH

The luminosity of a zero-age horizontal branch (ZAHB) star is derived from He core burning and H shell burning, the luminosities of which increase with the core mass M_c and the envelope mass M_{env}. The effective T_{eff} of a ZAHB star increases

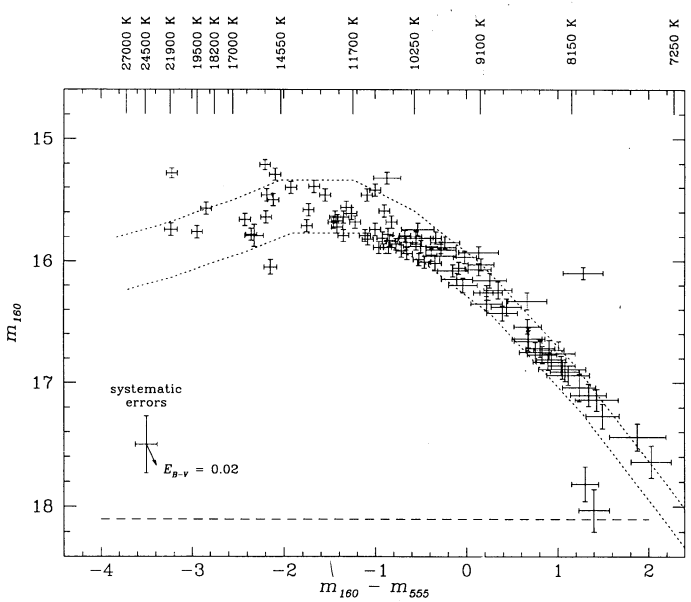

FIG. 2.—Far-UV to visible color-magnitude diagram for NGC 6681. The error bars denote random errors; systematic errors in the transformation to absolute magnitudes are about 0.23 in m_{160}, 0.12 in $m_{160} - m_{555}$, and 0.02 in E_{B-V}, and are shown in the lower left. Stars on the HB cooler than about 10,000 K are saturated in F555W and have larger error bars. The approximate limiting magnitude $m_{160} \approx 18.1$ is marked with a dashed line. The dotted lines are the [Fe/H] $= -1.48$ model ZAHB of Dorman, Rood, & O'Connell (1993) at the currently accepted DM of 14.82 and E_{B-V} of 0.06 (*upper curve*) and with the DM increased by 0.2 and E_{B-V} by 0.02 (*lower curve*). The temperatures along the top of the diagram correspond to the model effective temperatures for the upper curve.

as M_{env} decreases. HB stars hotter than $T_{eff} \approx 15{,}000$ K evolve at approximately constant T_{eff} as L_{bol} roughly doubles. The hottest star in the present CMD has $T_{eff} \approx 22{,}000$ K, corresponding to $M_{env} \approx 0.02\ M_{\odot}$ in the models of Dorman, Rood, & O'Connell (1993). He main-sequence stars (subdwarf O stars in the notation of Greenstein & Sargent 1974) are not present.

Post-HB evolution is complex, depends critically on a variety of parameters, is shorter in duration than the HB stage, and occurs at lower T_{eff}, with the exception of AGB-manqué stars which spend a time equal to approximately one-fifth of their HB lifetime at high temperatures and luminosities. The lack of stars brighter than $m_{160} = 15.0$ is an important constraint on post-HB stellar evolution, as we do not detect AGB-manqué (Greggio & Renzini 1990), post–early-AGB (Brocato et al. 1990), or post-AGB stars. Our failure to detect hot descendants of HB stars is consistent with our detection of only four stars with $T_{eff} > 16{,}000$ K (extreme-HB stars in the nomenclature of Dorman, Rood, & O'Connell 1993), likely progenitors of AGB-manqué and post–early-AGB stars, and the very short lives of post-AGB stars.

Also shown on the CMD is the [Fe/H] = −1.48 model ZAHB from Dorman, Rood, & O'Connell (1993), with preliminary synthetic magnitudes generated by Dorman (1994) from Kurucz (1991) model atmospheres and our preliminary response curves. Many stars fall below the model ZAHB at the currently accepted DM of 14.82 and E_{B-V} of 0.06 (the upper curve in the CMD). A much better fit is obtained if the DM is increased by 0.2 and E_{B-V} by 0.02 (the lower curve in the CMD). These shifts are within the informal uncertainties in DM and extinction, and the final fit is fully consistent with uncertainties in our preliminary synthetic magnitudes and colors. We are undertaking ground-based observations to formalize and reduce the uncertainties in the distance and extinction. The star with $m_{160} \approx 16.1$ and $m_{160} - m_{555} \approx 1.3$ is probably simply a star nearing the end of its life on the HB.

Even if the lower curve is adopted, one star still clearly falls below the model ZAHB. This star is about 20″ from the center of the cluster, making it unlikely to be a foreground object. UIT has found discrepancies between observations and model ZAHBs in other globular clusters (Hill et al. 1992; Parise et al. 1994; Whitney et al. 1994), although some uncertainties in calibration remain. It is not clear whether this single star is similar to those which fall below the model ZAHB in the UIT data or if it has a different origin.

One possibility that has not been widely discussed is that the core mass of stars evolving off the red giant branch might vary significantly within a cluster at a given time, allowing stars with lower core masses to appear below the envelope defined by those with higher core masses. This requires "noncanonical effects" such as rotation, nonconvective mixing, magnetic fields, or mass loss (Renzini 1977; Sweigert 1994). Mengel & Gross (1976) found that rotation might delay the He flash and allow larger cores.

4. BLUE STRAGGLERS

The CMD shows two fainter stars at $m_{160} \approx 18.0$, and $m_{160} - m_{555} \approx 1.4$. We have examined the original frames and conclude that these stars are indeed real. Their absolute magnitudes and colors are similar to those of late main sequence A stars, and we suspect that they are hot blue stragglers or possibly cataclysmic variables. They are located within 2″ of the center of the cluster. Although they are at the bright end of the luminosity function of Sarajedini & DaCosta (1991), similar stars have been found in the centers of 47 Tuc by Paresce et al. (1991) and Guhathakurta et al. (1992) and NGC 6397 by Lauzeral et al. (1992).

5. THE RADIAL PROFILE

Figure 3 shows radial number density profiles for the hot HB stars and bright giants (defined by saturation in F555W and absence in F160W). These were calculated using annuli whose inner and outer radii differ by 0.3 in log r, except the first point, which refers to a disk of radius 0.3 in log r. Only stars on the WFs were included. The center was determined by iteratively calculating the centroid of the bright giants in a 7″.5 aperture. Figure 3 also shows the U surface brightness profile from CCD photometry by Lugger, Cohn, & Grindlay (1995) scaled to match the number density profiles at large radii. The U band includes contributions from giants, main-sequence stars near the turnoff, and HB stars.

Although the profile for the hot HB stars is suggestive of a core, we caution against overinterpretation: there are only two hot HB stars and six bright giants in our inner bin. The excellent agreement between the profiles indicates a high level of consistency in and between the data sets. The data are in contrast to the far-UV radial gradients found by Djorgovski & Piotto (1992) in two other post–core-collapse clusters. The profiles of "red" and "blue" hot HB stars (divided on the basis of saturation in F555W) were also found to agree to within statistical errors.

We estimate that there are a total of 206 ± 20 hot HB stars in the cluster, based on the number within the half-light radius of 43″ (Trager, Djorgovski, & King 1993) with an uncertainty from Poisson statistics.

6. SUMMARY

We have obtained far-UV images of the globular cluster NGC 6681. We easily resolve all of the hot HB stars in the field. We have constructed a far-UV to visible color-magnitude diagram for the hot HB and find no evidence for hot descendants beyond core He exhaustion. With the exception of one star and within observational uncertainties, we find agreement with the ZAHB models of Dorman, Rood, & O'Connell (1993). These observations are a promising demonstration of the

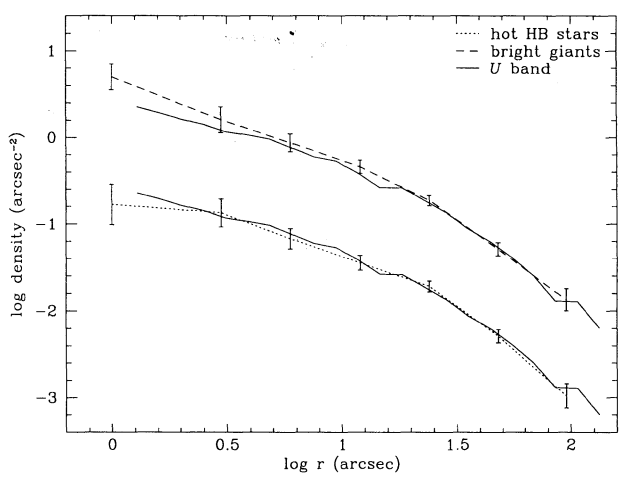

FIG. 3.—Radial density profiles for NGC 6681. The lower, dotted line is the radial projected number density profile of hot HB stars and the upper, dashed line is the radial projected number density profile of bright giants shifted up to 1 in the log for clarity. The 1 σ error bars are from Poisson statistics. The solid lines are the U surface brightness density profile of Lugger, Cohn, & Grindlay (1995) scaled to match the number density profiles at large radii.

unique ability of WFPC2 to study hot evolved stars in globular clusters.

Based on our experience with these images, we suggest that long exposures with F160W should be "CR-split" into more than two exposures to provide better discrimination against cosmic rays. We estimate that the 5 σ limiting magnitude attained from four 1000 s exposures is $m_{160} \approx 20.5$ near the center and $m_{160} \approx 20.0$ near the edge of the WFs.

The success of WFPC2 has been made possible by the dedicated efforts of many people, including the project engineering staff at JPL and the flight and support crew of STS-61. We are grateful to Ben Dorman for producing synthetic magnitudes at short notice, to Bob Rood and again Ben Dorman for valuable discussions and comments on earlier versions of the manuscript, to Haldan Cohn for the U surface brightness profile, to Mark Clampin for the spectrum of GRW +70°5824, to Ron Gilliland for a copy of his paper prior to submission, and to an anonymous referee for several useful suggestions. This research has made use of the Simbad database, operated by CDS, Strasbourg, France, and was carried out by the WFPC2 Science Team for JPL with the support of NASA contract NAS 7-1260.

REFERENCES

Brocato, E., Matteucci, F., Mazzitelli, I., & Tornambé, A. 1990, ApJ, 349, 458
Burrows, C. J. 1994, WFPC2 Instrument Handbook (2d ed.; Baltimore: STScI)
Caloi, V., Castellani, V., Galluccio, D., & Wamsteker, W. 1984, A&A, 138, 485
Cardelli, J. A., Clayton, G. C., & Mathis, J. S. 1989, ApJ, 345, 245
Djorgovski, S. G., & King, I. R. 1984, ApJ, 277, L41
Djorgovski, S. G., & Piotto, G. 1992, AJ, 104, 2112
Dorman, B. 1994, private communication
Dorman, B., Rood, R. T., & O'Connell, R. W. 1993, ApJ, 419, 596
Gilliland, R. L. 1994, ApJ, 435, L63
Greenstein, J., & Sargent, A. 1974, ApJS, 28, 157
Greggio, L., & Renzini, A. 1990, ApJ, 364, 35
Guhathakurta, P., Yanny, B., Schneider, D. P., & Bahcall, J. N. 1992, AJ, 104, 1790
Hill, R. S., et al. 1992, ApJ, 395, L17
Holtzman, J. A., Hester, J. J., Casertano, S., & WFPC2 Investigation Definition Team, 1994, Draft WFPC2 Status Report
Kurucz, R. L. 1991, in Precision Photometry: Astrophysics of the Galaxy, ed. A. G. D. Philip, A. R. Upgren, & K. A. Janes (Schenectady: Davis), 27
Landsman, W. B., et al. 1992, ApJ, 395, L21
Lauzeral, C., Ortolani, S., Aurière, M., & Melnick, J. 1992, A&A, 262, 63
Lugger, P. M., Cohn, H. N., & Grindlay, J. E. 1995, ApJ, in press
Mengel, J. G., & Gross, P. G. 1976, Ap&SS, 41, 407
O'Connell, R. W. 1993, in The Globular Cluster-Galaxy Connection, ed. G. H. Smith & J. P. Brodie (San Francisco: ASP), 530
Paresce, F., et al. 1991, Nature, 352, 297
Parise, R. A., et al. 1994, ApJ, 423, 305
Peterson, C. J. 1993, in Structure and Dynamics of Globular Clusters, ed. S. G. Djorgovski & G. Meylan (San Francisco: ASP), 337
Renzini, A. 1977, in Advanced Stages in Stellar Evolution, ed. P. Bouvier & A. Maeder (Geneva: Geneva Obs.), 149
Sarajedini, A., & DaCosta, D. G. 1991, AJ, 102, 628
Smith, E. P., et al. 1993, ApJ, 418, 850
Sweigert, A. V. 1994, ApJ, 462, 612
Trager, S. C., Djorgovski, S., & King, I. R. 1993, in Structure and Dynamics of Globular Cluster, ed. S. G. Djorgovski & G. Meylan (San Francisco: ASP), 347
Trauger, J. T., et al. 1994, ApJ, 435, L3
Turnshek, D. A., Bohlin, R. C., Williamson, R. L., Lupie, O. L., Koornneef, J., & Morgan, D. H. 1990, AJ, 99, 1243
van Albada, T. S., de Boer, K. S., & Dickens, R. J. 1981, MNRAS, 195, 591
Whitney, J. H., et al. 1994, AJ, in press
Zinn, R., & West, M. 1984, ApJS, 55, 45

1994ApJ...435L..55W

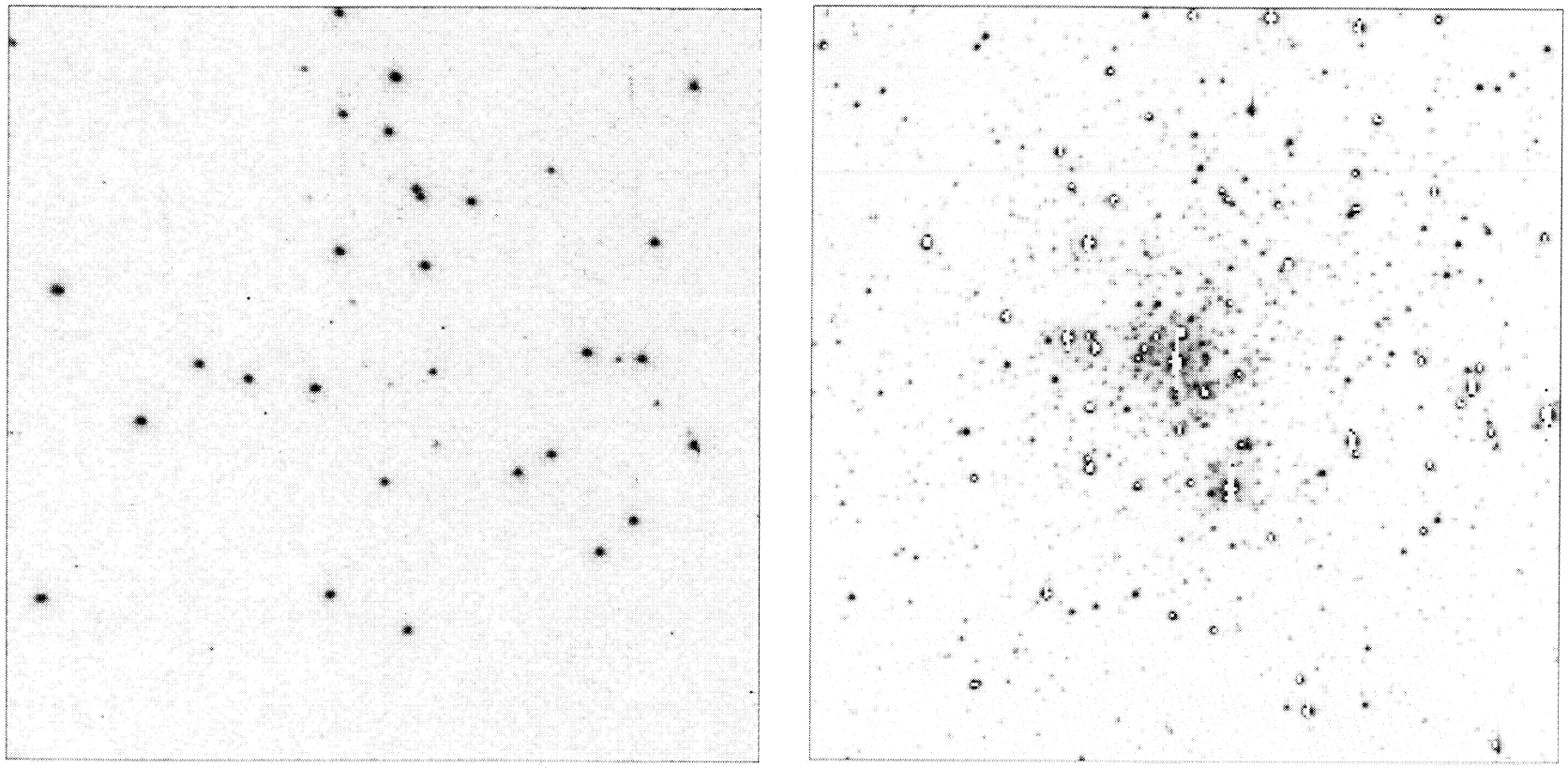

FIG. 1.—Far-UV F160W (*left*) and visible F555W (*right*) images of the center of NGC 6681. The images are 25".6 to a side at a pixel scale of 0".1 and have negative logarithmic intensity scales. The rotation between these and celestial coordinates is 37°.1, with north roughly to the upper right and east roughly to the upper left. Saturated pixels in the F555W image are white.

WATSON et al. (see 435, L55)